1 of 1

Fiber optic temperature sensor using a
Y_2O_2S:Eu thermographic phosphor

Todd V. Smith

Department of Physics, Bethel College
3900 Bethel Drive, St. Paul, Minnesota 55112

D. Barton Smith

Engineering Technology Division, Oak Ridge National Laboratory
P.O. Box 2003, Oak Ridge, Tennessee 37831-7280

ABSTRACT

This report details the development and testing of a thermographic-phosphor-based fiber-optic temperature sensor. The sensor is constructed by removing a region of the fiber jacket and cladding, then coating the exposed core with yttrium oxysulfide doped with a europium activator (Y_2O_2S:Eu). When photoexcited, the europium in the host lattice emits a sharp-line fluorescence spectrum that is characteristic of the temperature of the host crystal lattice. By measuring fluorescence lifetimes, we can deduce the temperature of an optical fiber that is in thermal contact with the fiber. Two different distributions of Y_2O_2S:Eu in the cladding region were evaluated with regard to light coupling efficiency. Theoretical waveguide calculations indicate that a thin core/cladding boundary distribution of Y_2O_2S:Eu couples light more efficiently into the cores guided modes than does a bulk distribution of phosphor in the cladding. The sensor tests showed reproducible response from 20 to 180 degrees Celsius. This technique has several advantages over other fiber optic temperature sensing techniques: the temperature measurement is independent of the strain applied to the fiber; the measurements are potentially accurate to within half a degree centigrade; the sensor allows temperature to be measured at precise locations; and the method doesn't preclude the use of the fiber for the simultaneous measurement of other parameters.

1. INTRODUCTION

Fiber optic sensing is a rapidly growing field with distinct advantages over other remote sensing techniques. Fiber sensors embedded in ceramic and composite parts can temperature and strain in the parts during the curing process and throughout their lifetime.

Many fiber optic temperature sensors have inherent problems or weaknesses that limit their effectiveness. Reflective methods[1] as well as Raman and doped core backscattering techniques[2] are not independent of strain. Interferometric methods are extremely sensitive which makes them susceptible to vibrations and other physical parameters.[3] These methods are expensive to implement, require complicated data analysis, and are difficult to calibrate. Optical Time Domain Reflectometry (OTDR) techniques cannot distinguish between fiber kinks or bends and temperature effects. They also require special equipment and are therefore expensive. Fibers with fluorescent materials on the tip provide a measurement at only one location.[4] OTDR backscattering techniques provide only marginal spatial resolution.[2]

The fiber optic temperature sensor design we report is an alternative to designs that use interference effects. It is an extrinsic quasi-distributed sensor.[5] The temperature sensitive material in the cladding region

is a thermographic phosphor, yttrium oxysulfide with 0.1% europium dopant. The use of rare-earth thermographic phosphors for temperature measurements is a mature sensing technology.[1,6-10] Recently, theoretical and experimental studies have been conducted on evanescent wave fluorosensors, which entail doping the cladding region with a sensing phosphor.[11-13] Luxtron Corporation has integrated phosphor and optical fiber technology in the form of a commercial temperature probe.[4]

When the phosphor is illuminated with ultraviolet (UV) light, the dopant ion electrons are excited into higher energy states and fluoresce as they relax to lower lying states. As the phosphor temperature changes the relaxation mechanisms change, resulting in a temperature dependent sharp-line emission spectrum. Figure 1 shows the emission spectrum for $Y_2O_2S:Eu$ at room temperature. The temperature of the phosphor can be deduced from the fluorescence lifetime of an emission line that has a strongly temperature dependent decay lifetime. Fonger and Struck provide a complete description of the characteristics of Eu^{3+} activated phosphors.[15]

We constructed the sensor by stripping and etching a small region of the jacket and cladding of the sensing fiber and coating the exposed core with a thin layer of the phosphor (Fig. 2). This provides a core/cladding boundary distribution of the phosphor. Ultraviolet light (337 nm) from a pulsed nitrogen gas laser propagates along the fiber and excites the phosphor. $Y_2O_2S:Eu$ has strong emission lines at 514 nm and 538 nm that have temperature dependent decay lifetimes. Using narrow band filters that pass only these wavelengths, a photomultiplier tube, a digital oscilloscope and a personal computer, phosphor emission decay signals from 20 to 180°C were captured and decay lifetimes were calculated.

Theoretical calculations based on work done by Egalon[11] and Marcuse[12] supported their conclusion that a distributions light sources, such as excited $Y_2O_2S:Eu$, located at the core/cladding interface would be more efficient at coupling light into the core of the fiber than would a bulk distribution of light sources throughout the cladding. However, more efficient coupling does not necessarily infer a larger signal. That is, the bulk distribution of light sources in the cladding could produce a larger signal even though light coupling is less efficient if the total light emitted is greater.

2. FABRICATION OF SENSOR

The fiber chosen for the sensor was Fiberguide Industries Superguide G UV-Vis fiber SFS400/480T with a pure fused silica core, doped fused silica cladding and thermocoat (polyimide) jacket. The 400 μm diameter core was chosen for its larger light guiding capacity and strength and the thermocoat jacket withstands temperatures in the range -190 to 385°C. The fiber also resists organic solvents which makes it attractive for embedding.[16] The final experimental configuration required the preparation of two fibers in order to make proper background measurements. The thermocoat jacket was removed from the ends (2-3 cm) of both fibers and the center (4-5 cm) of the sensing fiber. The ends of both fibers were cleaved and polished. Next a small region of the cladding was removed from the center of the sensor. A very small amount of Sperex SP-115 clear high temperature binder was applied to the etched region, and the phosphor, in powder form, was applied to the binder (Fig. 2). After the binder hardened, a capillary tube was slipped over the sensing region to provide strength to the weakened area.

3. EXPERIMENTAL LAYOUT

The experimental layout is shown in Fig. 3. The output from a PRA model LN1000 pulsed nitrogen laser was turned by a 337-nm beam splitting dichroic mirror and focused with an f-number matching UV grade lens onto the end of the background fiber. The other end of the background fiber was lined up with
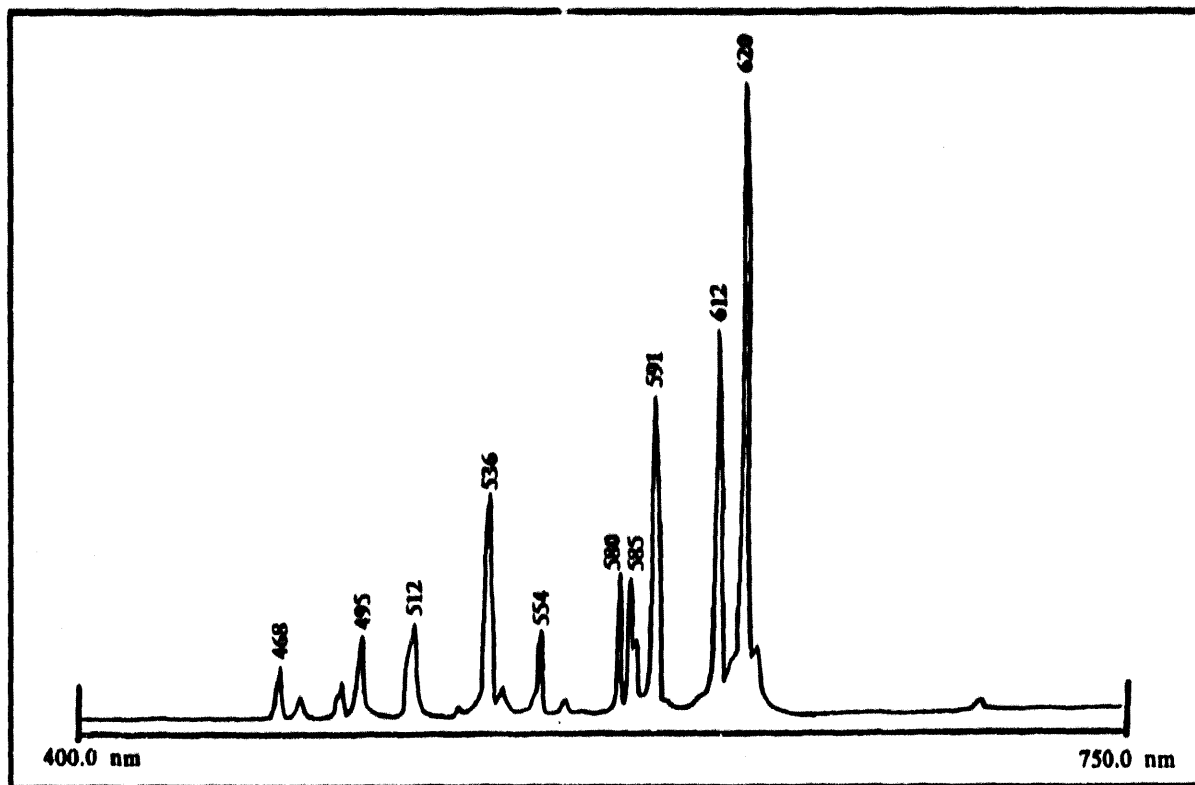
Fig. 1. Room temperature emission spectrum of Y_2O_2S:Eu with 355-nm excitation (from Ref. 13). The emission spectrum with 337-nm excitation is essentially identical. The emission intensity is plotted as a function of wavelength.
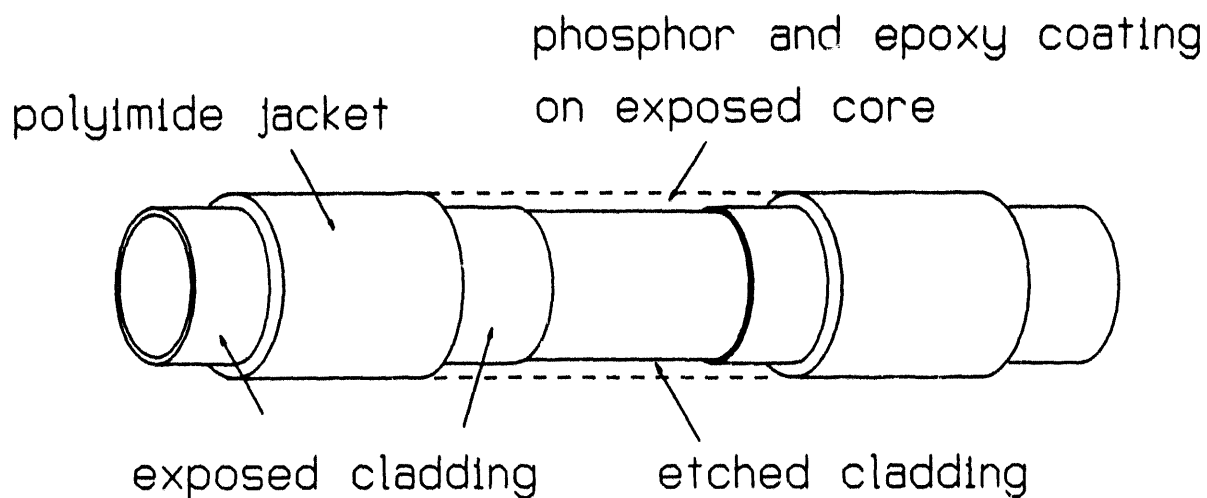

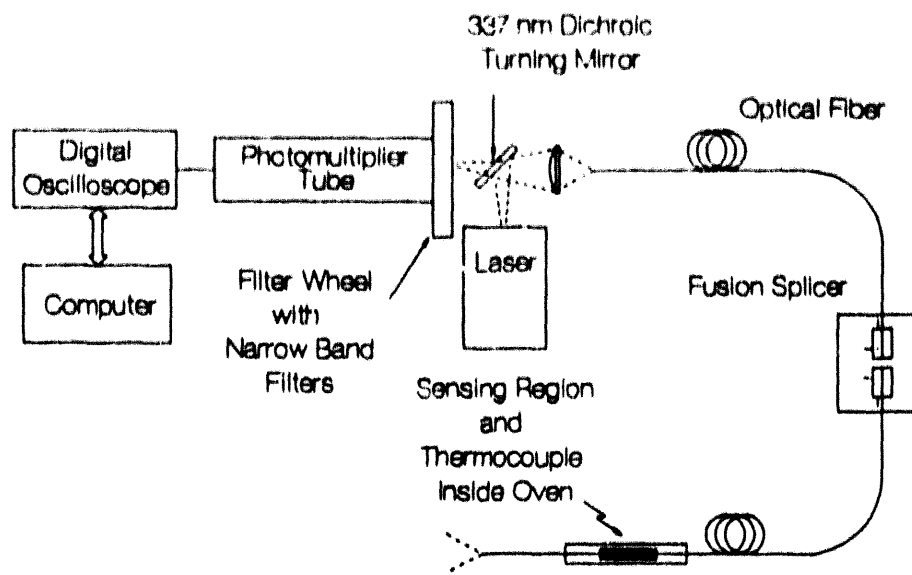Fig. 2. Diagram of optical fiber sensor sensing region.

Fig. 3. Experimental layout for testing the thermographic-phosphor-based fiber-optic temperature sensor.
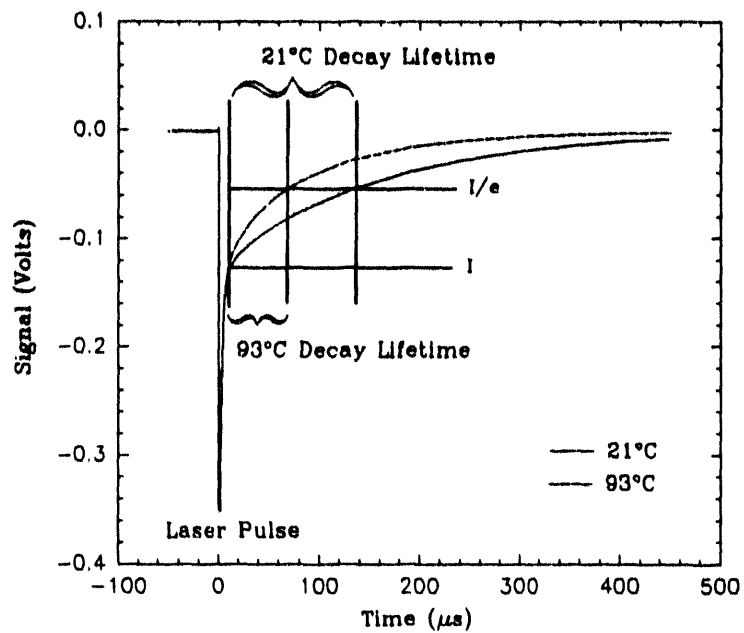

Fig. 4. Fluorescence decay of the 538-nm emission line at 21°C and 93°C.

the sensing fiber using micron adjustable alignment stages. The ultraviolet light propagating through the core excited the phosphor in the sensing region, which was located at the center of copper tube oven. The temperature at the center of the tube is continuously measured by a type-K thermocouple and thermocouple meter.

The fluorescence emission propagates along the fiber in both directions. A filter wheel with 514-nm and 538-nm narrow band filters was mounted to the front of an photomultiplier tube just behind the dichroic mirror. This configuration was chosen because the noise from the laser superradiance was smaller behind the mirror than at the other end of the fiber. Also, this allowed us to take background measurements by simply translating the two fibers off axis with the fusion splicer stages. Launch and exit conditions remained constant. The signal from the photomultiplier tube was measured by a digitizing oscilloscope. 100 successive signals were averaged and transferred to a computer where the data was manipulated, analyzed and graphed as lifetime versus temperature. A Mathcad® program was used to determine the decay lifetime from the waveform measured by the oscilloscope.

The simplest mathematical of the fluorescence signal is a single exponential decay, written as

$$I(t) = I_0 e^{-t/\tau} , \tag{1}$$

where I(t) is intensity of the fluorescent signal, I_0 is this signal at time equals 0, t is time, and τ, the decay lifetime, is the time it takes for the signal to drop from I_0 to I_0/e. This equation can be solved for τ by two methods. In one method called the natural log slope method, the natural log of each intensity value is computed. Then the linear regression of the resulting waveform is calculated. τ equals the negative reciprocal of the regression slope, that is

$$\tau = \frac{-1}{\dfrac{d}{dt}\ln[I(t)]} . \tag{2}$$

In another method, the decay signal is numerically integrated and divided by the lower limit signal minus the upper limit signal. This method can be expressed as

$$\tau = \frac{\displaystyle\int_{t_1}^{t_2} I(t)dt}{I(t_1) - I(t_2)} . \tag{3}$$

4. EXPERIMENT

Separate runs of data were taken to determine the stability and reproducibility of the temperature sensor measurements. The fibers were translated off axis at the splicer, and background measurements were taken with both phosphors. The background readings eliminate any error that might occur due to reflections from the mirror, lens and background fiber. Background measurements were constant over temperature range. Sensing fiber reflections, and binder and sensing fiber jacket fluorescence were inseparable from the

signal but were assumed to be negligible. Next, the fibers were aligned and phosphor readings were taken. After the temperature stabilized, one decay waveform for each wavelength was acquired. The oven was set for the next temperature and the process was repeated. Measurements were made while increasing the temperature and then again with decreasing temperature.

5. RESULTS

Figure 4 shows fluorescence decay signals at 21 and 93°C. The difference in lifetime between the two temperatures is clearly evident.

The temperature dependence of the fiber sensor is shown in Figs. 5 and 6. The different sets of data denote different test runs and indicate that the results are reproducible. The slope shows that the sensor signal has a logarithmic dependence on temperature.

6. CONCLUSIONS

The experimental configuration and technique described produces reproducible temperature dependance. In the future we see this technique expanded to larger temperature ranges, multiple sensing regions on a single fiber, and embedment within ceramics and composites. Phosphor sensors have been used to measure temperatures from -200 to 1800°C so this sensor's range is limited only by the temperature range of the fiber itself.[10] Luxtron reports phosphor temperature measurements accurate to 0.1°C.[4] This sensor is very robust and inexpensive unlike many interferometric and OTDR systems. The sensor is insensitive to vibration and microbending losses. Since the temperature information is contained in the shape of the decay waveform, our measurements are transmission loss independent. Extraction of temperature information involves simple equipment and calculations. The spatial resolution of the temperature measurement is 4-5 cm, the length of the sensor. This allows us to measure temperatures at precise locations through careful placement of the fiber.

Since the core is not broken we have the opportunity to construct additional sensing regions at other positions along the fiber. This could be done with the use of several different phosphors with different temperature dependent spectral lines. Multimode dispersion, which would change the decay time of the fluorescence signal, may limit the total length of the sensor. We also foresee using the fiber to simultaneously measure strain or some other parameter of interest using OTDR or interferometric techniques.

A lower loss connection between the sensing fiber and the background fiber would improve sensitivity by increasing signal size and decreasing reflection noise. Due to the intensity of the 600 picosecond laser pulse and superradiance, the photomultiplier tube becomes overloaded, requiring some recovery time. This is possibly a hinderance to our measurements of the shortest lifetimes (on the order of a microsecond). A possible next step for this technique is switching to a smaller fiber. For sensing purposes, in order to be less intrusive, the smaller the fiber the better. However as discussed in the results, a larger fiber has a larger light guiding capacity. This affects both excitation and emission light since the higher order modes of the excitation light penetrate deeper into the cladding resulting in a larger fluorescence signal. Theoretical calculations provide a way to evaluate potential sensing fibers and fiber/phosphor configurations. The present configuration includes a capillary tube jacket around the sensing region. This adds size and thermal mass, but without it the etched region is extremely brittle and would be more so in a smaller fiber. Fibers drawn with segments of phosphor at the core/cladding interface would alleviate this problem.

7. ACKNOWLEDGMENTS

8. REFERENCES

1. D. A. Krohn, Fiber Optic Sensors: Fundamentals and Applications, Ch. 7, Instrument Society of America, Research Triangle Park, NC, 1988.

2. A. A. Boiarski, "Distributed Fiber Optic Temperature Sensing," Applications of Fiber Optic Sensors in Engineering Mechanics, ed. Farhad Ansari, American Society of Civil Engineers, New York, 1993.

3. Anthony Dandridge, "Fiber Optic Sensors Based on the Mach-Zehnder and Michelson Interferometers," Fiber Optic Sensors: An Introduction for Engineers and Scientists, ed. Eric Udd, pp. 271-320, John Wiley & Sons, Inc., New York, 1991.

4. K. A. Wickersheim and M. H. Sun, "Fluoroptic Thermometry," Medical Electronics, pp. 84-91, February 1987.

5. Alan D. Kersey, "Distributed and Multiplexed Fiber Optic Sensors," Fiber Optic Sensors: An Introduction for Engineers and Scientists, ed. Eric Udd, pp. 325-340, John Wiley & Sons, Inc., New York, 1991.

6. J. W. Berthold III, "Industrial Applications of Fiber Optic Sensors," Fiber Optic Sensors: An Introduction for Engineers and Scientists, ed. Eric Udd, pp. 413-419, John Wiley & Sons, Inc., New York, 1991.

7. K. W. Tobin et al., "Engine Testing of Thermographic Phosphors", ORNL/ATD-31, Martin Marietta Energy Systems, Inc., Oak Ridge Nat. Lab., 1990.

8. S. W. Allison et al., "Calibration of a Laser-Pumped, Thermographic Phosphor Remote Thermometry System," K/ETAC-8, Martin Marietta Energy Systems, Inc., Oak Ridge Gaseous Diffusion Plant, 1987.

9. S. W. Allison et al., "Rare-Earth Phosphors for Remote Thermographic Applications", ORNL/ATD-12, Martin Marietta Energy Systems, Inc., Oak Ridge Nat. Lab., 1989.

10. M. R. Cates, "New Light on Measuring Temperature," Oak Ridge National Laboratory Review, Vol. 24, Nos. 3 and 4, pp. 46-55, 1991.

11. C. O. Egalon and R. S. Rogowski, "Model of a thin film optical fluorosensor," SPIE Vol. 1368 Chemical, Biochemical, and Environmental Fiber Sensors II, pp. 134-149, 1990.

12. D. Marcuse, "Launching Light into Fiber Cores from Sources Located in the Cladding," Journal of Lightwave Technology Vol. 6 (8), pp. 1273-79, August 1988.

13. J. D. Andrade et al., "Remote Fiber-Optic Biosensors Based on Evanescent-Excited Fluoro-Immunoassay: Concept and Progress," IEEE Transactions on Electron Devices ED-32(7), pp. 1175-79, July 1985.

14. Alan R. Bugos, "Characterization of the Emission Properties of Thermographic Phosphors For Use in High Temperature Sensing Applications," M. S. Thesis, University of Tennessee, Knoxville, 1989 (unpublished).

15. W. H. Fonger and C. W. Struck, "Eu^{3+} ^5D Resonance Quenching to the Charge-Transfer States in Y_2O_2S, La_2O_2S, and $LaOCl$," J. Chem. Phys. 52, pp. 6364-6372, 1970.
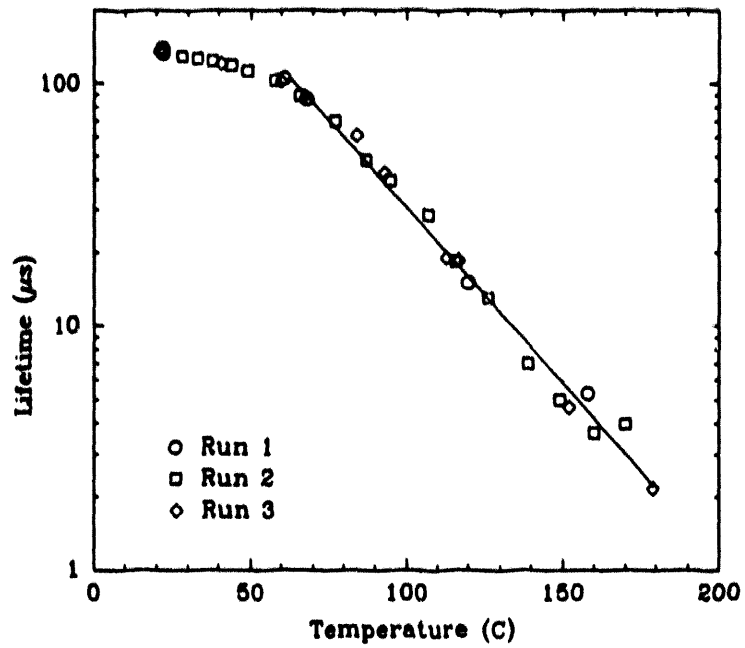
16. Fiberguide Industries, Inc., Stirling, NJ, 1991.

Fig. 5. Decay lifetime versus temperature for the 514-nm emission line.
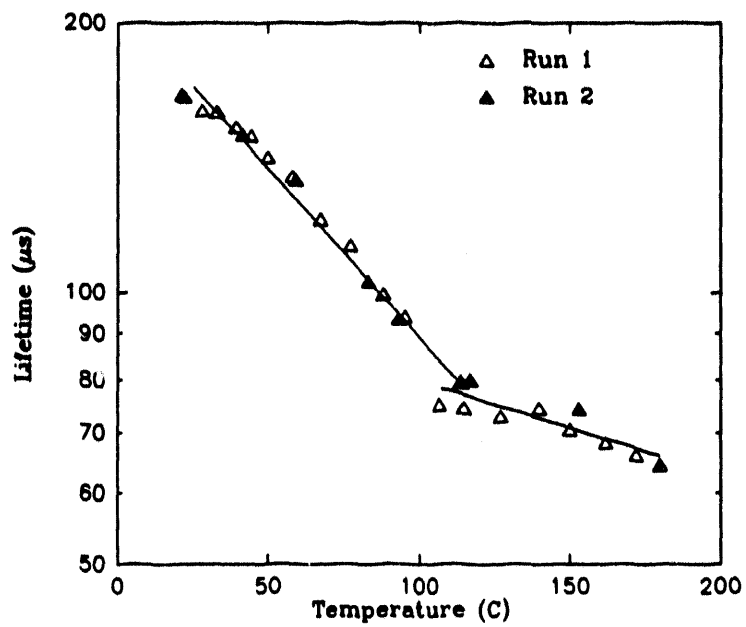

Fig. 6. Decay lifetime versus temperture for the 538-nm emission line.

DATE
FILMED
12 / 01 / 93

END